Clinical Science (2022) **136** 455–471
https://doi.org/10.1042/CS20211031

PORTLAND PRESS

Research Article

Inhibition of Notch activity suppresses hyperglycemia-augmented polarization of macrophages to the M1 phenotype and alleviates acute pancreatitis

Ning Hu[1,*], Xiaoyi Zhang[2,*], Xuanzhe Zhang[1], Yongjun Guan[1], Ruyuan He[3], Enfu Xue[1], Xiaoyi Zhang[4], Wenhong Deng[1], Jia Yu[1], Weixing Wang[1,5] and Qiao Shi[1,6,7]

[1]Department of General Surgery, Renmin Hospital of Wuhan University, Wuhan, China; [2]Department of Critical Care Medicine, Zhongnan Hospital of Wuhan University, Wuhan, China; [3]Department of Thoracic Surgery, Renmin Hospital of Wuhan University, Wuhan, China; [4]Department of Gynecology and Obstetrics, Renmin Hospital of Wuhan University, Wuhan, China; [5]Key Laboratory of Hubei Province for Digestive System Disease, Renmin Hospital of Wuhan University, Wuhan, China; [6]Department of Pancreatic Surgery, Renmin Hospital of Wuhan University, Wuhan, China; [7]Central Laboratory, Renmin Hospital of Wuhan University, Wuhan, China

Correspondence: Weixing Wang (sate.llite@163.com) or Qiao Shi (shiqiao614@163.com)

Acute pancreatitis (AP) is an acute inflammatory disorder characterized by acinar cell death and inflammation. Multiple factors cause hyperglycemia after AP. Macrophage polarization is involved in tissue injury and repair, and is regulated by Notch signaling during certain inflammatory diseases. The present study explores the relationship among hyperglycemia, macrophage polarization, and Notch signaling during AP and the related mechanisms. A cerulein-induced AP model was established in FVB/N mice, and AP with hyperglycemia was initiated by injection of 50% concentration glucose. Tissue damage, Notch activity, and macrophage polarization were assessed in pancreatic tissues. The role of Notch signaling in macrophage polarization during AP was also assessed *in vitro* by co-culturing primary macrophages and pancreatic acinar cells, and establishing a lipopolysaccharide (LPS)-induced inflammatory model in RAW264.7 cells. Pancreatic acinar cells were damaged and proinflammatory factor levels were increased in pancreatic tissues during AP. The hyperglycemic conditions aggravated pancreatic injury, increased macrophage infiltration, promoted macrophage polarization towards an M1 phenotype, and led to excessive up-regulation of Notch activity. Inhibition of Notch signaling by DAPT or Notch1 knockdown decreased the proportion of M1 macrophages and reduced the production of proinflammatory factors, thus mitigating pancreatic injury. These findings suggest that hyperglycemia induces excessive Notch signaling after AP and further aggravates AP by promoting pancreatic macrophage polarization towards the M1 phenotype. The Notch signaling pathway is a potential target for the prevention and treatment of AP.

[*]These authors contributed equally to this work.

Received: 03 November 2021
Revised: 16 March 2022
Accepted: 18 March 2022

Accepted Manuscript online: 18 March 2022
Version of Record published: 06 April 2022

Introduction

Acute pancreatitis (AP), characterized by acinar cell death and local or systemic inflammation, is the most common pancreatic disease [1]. The global incidence of AP is currently 33.74/100000 person-years and has been increasing worldwide [2,3]. It is critical to prevent AP from developing into severe disease, which is associated with multiple organ dysfunction and increased mortality [4]. In spite of progress in the development of AP treatment strategies over the past few decades, there are still no effective therapeutic medications to mitigate disease progression [3,5,6].

Clinical Science (2022) **136** 455–471
https://doi.org/10.1042/CS20211031

In clinical practice, most AP patients have elevated and fluctuating blood glucose levels, which may be due to stress response, β-cell injury, and nutritional treatment [7–10]. A previous study showed that diabetes is associated with an increased risk of severe AP [11]. However, whether hyperglycemic conditions and fluctuating blood glucose observed in the early phase of AP exacerbate pancreatic injury remains unclear.

During tissue injury and infection, monocytes migrate to tissues and differentiate into macrophages [12]. This cell type has two phenotypes: M1 macrophages represent the proinflammatory state and are characterized by iNOS expression and production of proinflammatory cytokines like interleukin (IL)-1β (IL-1β), IL-6, and tumor necrosis factor-α (TNF-α), while M2 macrophages represent the anti-inflammatory state and are characterized by the production of IL-10 [13]. M1 macrophages dominate the proinflammatory phase of AP, while M2 macrophages dominate the phase of pancreatic repair and regeneration [14]. Diabetes is associated with tissue injury and inflammation in multiple organs [15,16], and a recent study showed that hyperglycemia during type 1 diabetes can aggravate acute liver injury by promoting the activation of liver-resident macrophages [17]. However, whether a hyperglycemic condition that follows AP would affect the polarization of pancreatic macrophages remains unknown.

The Notch signaling pathway is relatively conserved, primarily regulating embryonic development, multiple cell lineage differentiation, and adult tissue homeostasis [18]. The Notch receptors, Notch 1–4, are produced in the endoplasmic reticulum (ER) and interact with the Notch ligands, Delta, Jagged, and Serrate, on the surface of adjacent cells [19]. When the Notch pathway is activated, the Notch intracellular domain (NICD) becomes liberated and translocates into the cell nucleus, where it binds to the DNA-binding protein, Rbpj [20,21]. This interaction results in the transcription of Notch downstream targets, such as Hes and Hey family genes [22]. Notch-Rbpj signaling plays an important role in macrophage development, activation, and polarization [23,24]. In a diabetic retinopathy model, the Notch1 ligands, Jagged1 and Delta Like-4, are up-regulated during hyperglycemia and activate Notch signaling [25]. However, it remains unknown whether hyperglycemia uses Notch signaling to regulate macrophage polarization and pancreatic injury during AP.

Materials and methods

Animal experiments

Animal experiments were approved by the Institutional Review Board of Renmin Hospital of Wuhan University (WDRM 20190108). FVB/N mice were purchased from Beijing Vital River Laboratory Animal Technology Co., Ltd (Beijing, China) and housed in pathogen-free conditions with free access to standard rodent chow and water. All animal experiments were performed in the Animal Experiment Center of Renmin Hospital of Wuhan University in accordance with standard guidelines. The AP model was established in 8–12-week FVB/N male mice using hourly intraperitoneal injections of cerulein (100 μg/kg body weight, C9026, Sigma–Aldrich, U.S.A.) six-times a day for 4 days [14,26]. Control mice (CON) were intraperitoneally injected with 0.9% saline. The AP with hyperglycemia group (APG) was induced after establishing the AP model using repeated intraperitoneal injections of 50% glucose (4 g/kg) 3 h apart, four-times per day for 1 week. The control with hyperglycemia group (CONG) was established using intraperitoneal injections of 50% glucose in control mice. Blood glucose levels were measured 1, 3, and 7 days after intraperitoneal injection of 50% glucose (4 g/kg) or saline. In detail, blood glucose levels were measured 0, 15, 30, 60, 90, and 120 min following glucose or saline injection with a glucometer (OneTouch UltraVue, Johnson & Johnson, U.S.A.) through the tail vein. Animals were killed at 1, 3, and 7 days after establishing the AP model. The mice were anesthetized using isoflurane inhalation before sample collection. Blood was obtained through the inferior vena cava, after which the mice died spontaneously, and their pancreases were immediately removed. Killing was confirmed using cervical dislocation. Pancreatic tissues were fixed in 4% paraformaldehyde or stored at −80°C for further histological and biochemical analyses.

Isolation of bone marrow-derived macrophages

FVB/N mice were killed by cervical dislocation and sterilized by immersion in 75% ethanol. The femurs and tibias were prepared under sterile conditions. Bone marrow was flushed out of the bones using sterile Dulbecco's modified Eagle's medium (DMEM) (G4520, Servicebio, China), the cells were incubated in sterile erythrocyte lysate for 10 min to remove red blood cells, passed through a cell strainer (70 μm), and collected in a 50-ml tube. The cells were then centrifuged for 10 min at 2000 *rpm* (5804R, Eppendorf, Germany), washed with sterile phosphate-buffered saline (PBS), and resuspended in low-glucose DMEM supplemented with 10% fetal bovine serum (FBS) (10999141, Gibco, Australia), 1% Penicillin–Streptomycin solution (P/S) (BL505A, BioSharp, China), and 20 ng/ml macrophage colony-stimulating factor (M-CSF) (315-02, PeproTech, U.S.A.), and maintained in a six-well culture plate. The cells were used for experiments 7 days after M-CSF stimulation [27].

Isolation of pancreatic acinar cells

Fresh pancreatic tissues were obtained from FVB/N mice and digested in type 1 collagenase (1.6 mg/ml, G0130, Sigma–Aldrich, U.S.A.) dissolved in 1× HBSS (BL561A, BioSharp, China) in a 37°C water bath for 20 min with gentle shaking. The enzymatic reaction was stopped with the addition of 1 mM $CaCl_2$. The digested tissue was centrifuged at 290×***g*** at 4°C for 2 min and washed twice with 1× HBSS. The pellet was resuspended and filtered through a 70-μm cell strainer to obtain dispersed acinar cells. Cells were cultured in low-glucose DMEM supplemented with 10% FBS and 1% P/S in 5% CO_2 at 37°C.

Cocultivation of bone marrow-derived macrophages and acinar cells

The acinar cells were washed with sterile PBS and maintained in six-well plates in fresh DMEM. Prior to cocultivation, acinar cells were stimulated with 100 nM cerulein for 12 h, washed with sterile PBS, and seeded on to cell culture inserts (0.4-μm pore size, 3412, Corning, U.S.A.). The inserts were transferred into the wells containing bone marrow-derived macrophages (BMDMs), and co-incubation was maintained for 4 days [28]. The cells were then incubated in DMEM supplemented with 5.5, 25, or 50 mM glucose. The γ-secretase inhibitor, DAPT (S2215, Selleck, U.S.A.), was added to the medium to inhibit Notch signaling. BMDM morphology was assessed using an inverted microscope.

Cell line, lentivirus transfection, and lipopolysaccharide treatment

Mouse macrophages from the RAW264.7 cell line (Procell Life Science & Technology Co., Ltd., China) were cultured in low-glucose DMEM containing 10% FBS and 1% P/S in 5% CO_2 at 37°C.

Lentivirus against Notch1 was obtained from Shanghai GeneChem Co., Ltd., China. Prior to transfection with lentivirus, RAW264.7 cells were seeded in 12-well plates at a 1×10^5 density per well, and fresh medium with lentivirus and HiTransG-P were added. After a 48-h transfection, 2 μg/ml puromycin (BS111, BioSharp, China) was added for the selection. After continuous selection with puromycin, the Notch1 knockdown RAW264.7 cell line was examined by Western blotting and quantitative real-time polymerase chain reaction (qRT-PCR). The lentivirus containing empty vector was used as a negative control. CON RAW264.7 cells and Notch1 knockdown RAW264.7 cells were stimulated with lipopolysaccharide (LPS) and cultured in DMEM with 5.5 or 50 mM glucose for 24 h. The cells were harvested for Western blotting and qRT-PCR analyses.

Histology

Pancreatic sections were stained with Hematoxylin and Eosin (H&E) and the severity of pancreatitis was analyzed by pathologic scoring. Injury indicators including edema, acinar necrosis, inflammation, perivascular infiltration, hemorrhage, and fat necrosis were analyzed by two researchers independently as described previously [29]. Edema, hemorrhage, and fat necrosis were assessed on whole tissue sections, while inflammatory infiltration, perivascular inflammation, and acinar necrosis were scored on ten 400× fields per slide.

Immunohistochemistry

The Elivision Super HRP IHC Kit (KIT99-22, MXB, China) was used for immunohistochemistry according to the manufacturer's instructions. Pancreatic sections were deparaffinized and rehydrated, and citrate buffer (pH 6.0, G1202, Servicebio, China) was used for antigen retrieval. Peroxidase blocking was performed in PBS with 3% H_2O_2 for 10 min, and permeabilization was conducted using 0.2% Triton X-100 (93443, Sigma–Aldrich, U.S.A.) for 45 min at room temperature. The slides were incubated with primary antibodies against IL-1β (1:200, GB11113, Servicebio), nuclear factor κ-B p65 (NF-κB p65) (1:200, GB11042, Servicebio), and Rbpj (1:200, 5313T, Cell Signaling Technology) overnight at 4°C. The slides were incubated with a response enhancer at 37°C for 20 min HRP-conjugated secondary antibody at 37°C for 20 min. AEC (ZLI-0936, ZSGB-Bio, China) or DAB (G1212, Servicebio, China) substrates were used for color development. Five sections in each group and ten 400× images per section were evaluated by calculating the number of positive cells/total number of cells.

Immunofluorescence

Pancreatic sections were deparaffinized and rehydrated. Tris-EDTA (pH 9.0, G1203, Servicebio, China) was used for antigen retrieval, 0.2% Triton X-100 was used for permeabilization, and 10% donkey serum was used for blocking. The sections were incubated with primary antibodies overnight at 4°C and incubated with secondary antibodies for 1 h at 37°C. For immunofluorescent staining, primary macrophages were fixed in 4% paraformaldehyde for 20 min and blocked in 10% donkey serum. Incubation with primary antibodies was performed overnight at 4°C. Secondary

Clinical Science (2022) **136** 455–471
https://doi.org/10.1042/CS20211031

antibody incubation was performed for 1 h at 37°C and DAPI (ab104139, Abcam, U.S.A.) was used to label the nuclei. The primary antibodies included CD68 (1:50, Sc-20060, Santa Cruz), iNOS (1:200, 18985-1-AP, Proteintech), CD206 (1:200, 18704-1-AP, Proteintech), IL-6 (1:200, GB11117, Servicebio), and Hes1 (1:200, ab108937, Abcam). The secondary antibodies included donkey anti-rabbit IgG H&L (Alexa Fluor® 488) (1:200, ab150073, Abcam), and donkey anti-mouse IgG H&L (Alexa Fluor® 594) (1:200, ab150108, Abcam). Five sections in each group were examined and ten 400× images per section were evaluated. $iNOS^+CD68^+$ cells represented M1 macrophages, $CD206^+CD68^+$ cells represented M2 macrophages, and $Hes1^+CD68^+$ cells represented Hes1-positive macrophages.

TUNEL staining

TUNEL staining was performed using the Click-iT Plus TUNEL Assay kit (C10618, Invitrogen, U.S.A.) with slight modifications in the manufacturer's instructions. Deparaffinized sections were immersed in 4% paraformaldehyde for 15 min at 37°C and washed twice with PBS. The slides were permeabilized with proteinase K for 15 min at 37°C. After incubation in 4% paraformaldehyde for 5 min, the sections were incubated with terminal deoxynucleotidyl transferase (TdT) reaction buffer for 10 min at 37°C. TdT reaction mixture (TdT reaction buffer, EdUTP, TdT enzyme) was added to the slides and incubated at 37°C for 1 h. The slides were rinsed with 3% BSA and 0.1% Triton X-100 in PBS and incubated in 1× Click-iT Plus TUNEL SuperMix for 30 min at 37°C. DAPI (ab104139, Abcam, U.S.A.) with mounting medium was used to label the nuclei. Five sections were examined in each group, and ten 400× images per section were evaluated to calculate TUNEL-positive cells/total cells.

Western blotting

Pancreatic tissue and cells were lysed in RIPA buffer (P0013B, Beyotime, China) containing proteinase, phosphatase inhibitor cocktail (04693132001 and 0490684500, Roche, Switzerland), and PMSF (G2008, Servicebio, China). The lysates were centrifuged at 12000 rpm (5424R, Eppendorf, Germany) and 4°C for 10 min to remove debris, and the supernatants were collected and used for electrophoresis. Ten percent silk milk was used for blocking. The primary antibodies included Hes1 (1:1000, 11988s, Cell Signaling Technology), Rbpj (1:1000, 5313T, Cell Signaling Technology), cleaved caspase-3 (1:1000, 9661T, Cell Signaling Technology), TNF-α (1:1000, GB11188, Servicebio), IL-6 (1:1000, 12912T, Cell Signaling Technology), iNOS (1:1000, 18985-1-AP, Proteintech), and GAPDH (1:1000, GB11002, Servicebio). Antigen–antibody complexes were probed with HRP-conjugated secondary antibody for 1 h at room temperature. Immunoproducts were detected using the Ultra-sensitive ECL Chemiluminescence Kit (BL523A, BioSharp, China).

qRT-PCR

Primary macrophages or RAW264.7 cells were homogenized in TRIzol reagent (G3013, Servicebio, China) for total RNA extraction. After incubation in TRIzol for 30 min at room temperature, the cells were scraped off the culture dish. Chloroform was added and mixed thoroughly, and the lysates were incubated at room temperature for 15 min and centrifuged for 10 min at 4°C. The supernatants were aspirated into fresh 1.5-ml EP tubes and precooled isopropanol was added. After incubation at 4°C for 15 min, the lysates were centrifuged at 12000 rpm (5424R, Eppendorf, Germany) for 10 min to obtain RNA products. The RNA products were washed three times with 75% ethanol and dissolved in 20 μl DEPC water (BL510A, BioSharp, China). The concentration of RNA was determined using Nanodrop 2000. RNA products were reverse transcribed into cDNAs using a GoScript reverse transcription system (K1691, Thermo Fisher, U.S.A.). The qRT-PCR was performed with SYBR Green reagent (G3320-01, Servicebio, China). Primer sequences for qRT-PCR are listed in Supplementary Table S1. Gene expression was normalized to GAPDH and analyzed using the $2^{-\Delta\Delta C_T}$ method.

Statistical analysis

Data are presented as mean ± SEM, and analyzed by SPSS 26.0 (IBM, U.S.A.) and Prism 8.0 software (GraphPad, U.S.A.). An unpaired Student's *t* test was used to evaluate the differences between two groups. $P<0.05$ was considered statistically significant.

Results

Hyperglycemia aggravates pancreatic injury during AP

A murine AP model was established through intraperitoneal injections of cerulein six-times a day for 4 days. After establishing the AP model, the hyperglycemic condition was created through intraperitoneal administration of 50% glucose (4 g/kg) for the indicated time period (Figure 1A). Significantly elevated blood glucose levels were observed

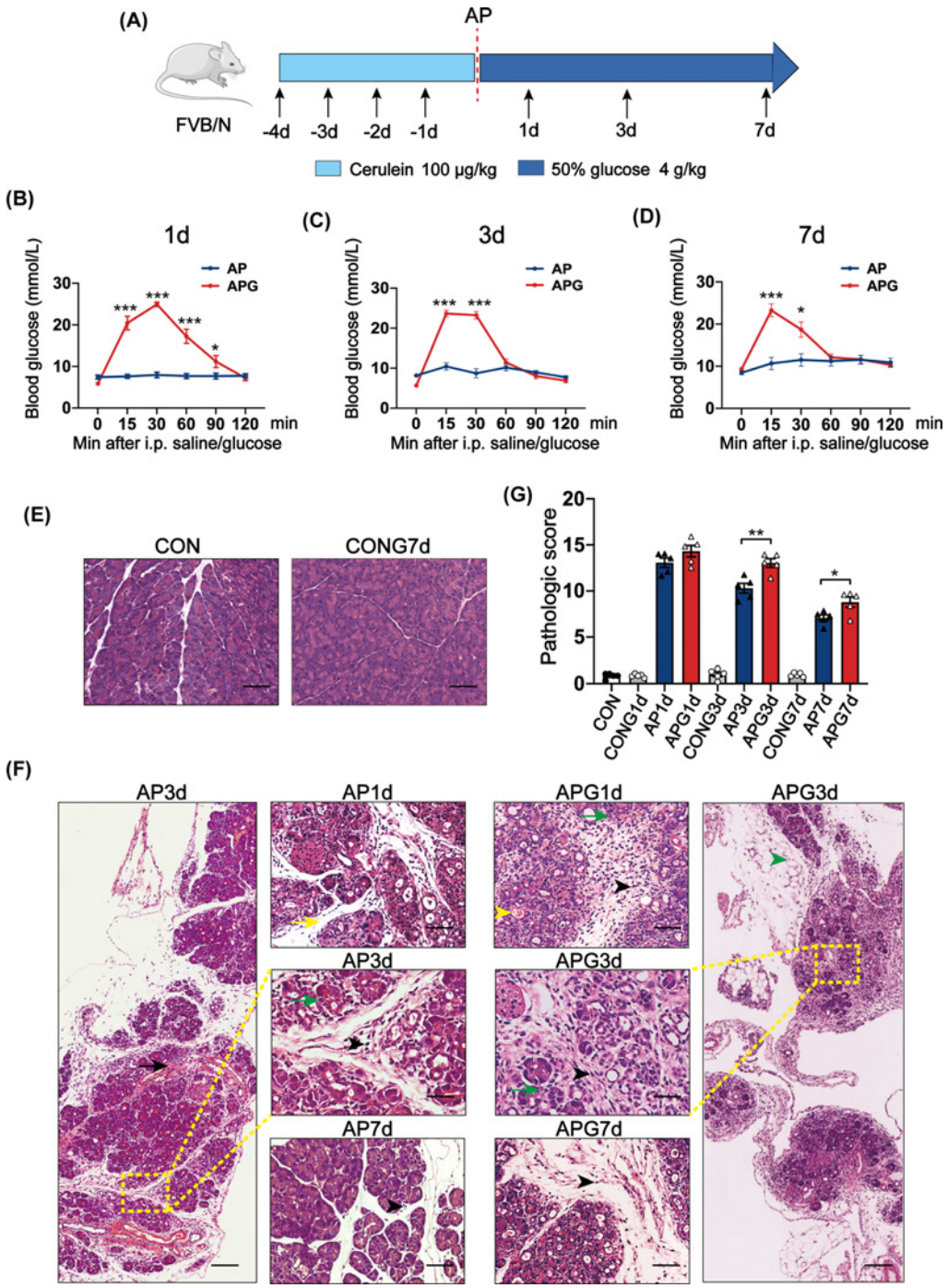

Figure 1. Hyperglycemia aggravates pancreatic injury following AP

(**A**) Schematic diagram of the animal model. (**B**–**D**) Changes in blood glucose in the AP and APG groups after saline/glucose injections 1, 3, and 7 days after AP. (**E**) Representative images of H&E staining of pancreases from CON and CONG mice. The CON and CONG images are from Supplementary Figure S1A,B, respectively. (**F**) Representative images of H&E staining of pancreases from AP and APG mice at indicated time points. The black arrowheads indicate inflammatory cells, including lymphocytes, monocytes, and macrophages, and the black arrows indicate perivascular inflammation. The yellow arrowheads indicate hemorrhage, and the yellow arrows indicate edema. The green arrowheads indicate fat necrosis, and the green arrows indicate necrotic acinar cells. The AP1d, APG1d, AP7d, and APG7d images are from Supplementary Figure S1C–F, respectively. (**G**) Pathological scores of pancreases in the CON, CONG, AP, and APG groups. Abbreviations: APG, acute pancreatitis with glucose treatment; CONG, control with glucose treatment. Data are presented as the mean ± SEM, n=5–8. *P<0.05, **P<0.01, ***P<0.001. Scale bars, 50 μm ((E) and middle panels of (F)) and 100 μm (left and right graphs of (F)).

Clinical Science (2022) **136** 455–471
https://doi.org/10.1042/CS20211031

following glucose injections 1, 3, and 7 days after AP (Figures 1B–D). The pancreases of non-AP mice that received glucose injections (CONG) were not different from those of control mice (CON) receiving saline (Figure 1E), indicating that the hyperglycemic condition did not injure the pancreas in the absence of pancreatitis. Compared with the normal pancreas structure observed in the CON group, obvious edema, acinar necrosis, and inflammatory cells infiltration were observed in pancreases from the AP group (Figure 1F). APG mice exhibited more severe pancreatic injury than AP mice at each indicated time point (Figure 1F,G). The detailed score for each pathological parameter in each group is listed in the Supplementary Table. These findings indicate that hyperglycemic conditions could aggravate pancreatic injury caused by AP.

Hyperglycemia exacerbates pancreatic inflammation and increases apoptosis following AP

To evaluate pancreatic inflammation in each group, IL-1β, NF-κB p65, and IL-6 expression was assessed by immunostaining and found to be significantly higher in the AP groups than in the CON groups. APG mice had higher levels of pancreatic inflammation than AP mice as shown by increased staining of IL-1β, NF-κB, and IL-6 at each time point (Figure 2A–F). Cleaved caspase-3 protein levels were also higher in pancreases from the AP group than those from the CON group. High-concentration glucose treatment resulted in a further increase in cleaved caspase-3, indicating that hyperglycemic conditions exacerbated apoptosis (Figure 2G,H). TUNEL staining also showed an increased number of apoptotic cells in APG mice than AP mice (Figure 2I,J). These findings suggest that hyperglycemia exacerbated pancreatic inflammation and increased cellular apoptosis during AP.

Hyperglycemia promotes pancreatic macrophage polarization towards an M1 phenotype following AP

The activation of pancreatic macrophages and their subphenotypes were examined by CD68, iNOS, and CD206 immunostaining in the pancreases of mice from each group. CD68 and iNOS costaining represented the proinflammatory M1 phenotype (Figure 3A), while CD68 and CD206 costaining represented the M2 phenotype (Figure 3B). Minimal expression of CD68 in the CON and CONG groups indicated that macrophages were not activated in the absence of pancreatitis. The injured pancreases of AP mice showed massive infiltration of CD68 positive macrophages, and this number further increased in mice receiving glucose insults (APG) (Figure 3C), suggesting that hyperglycemia facilitated macrophage activation. In addition, the proportion of each macrophage subtype differed between the AP and APG groups (Figure 3D). While both the AP1d and APG1d groups had a high proportion of M1 macrophages, the APG group had significantly more M1 macrophages than the AP group at days 3 and 7. In contrast, while M2 macrophages were activated in both the AP1d and APG1d groups, a significant increase in M2 macrophages was observed in the AP3d and APG3d groups. The APG7d group had significantly less M2 macrophage infiltration than the AP7d group. In addition, the ratio of M1 to M2 macrophages was higher in the APG than in the AP group on days 3 and 7 (Figure 3E). These data suggest that the hyperglycemic condition promoted differentiation of pancreatic macrophages towards an M1 phenotype and inhibited M2 polarization.

Notch activity is augmented under hyperglycemic conditions during AP and associated with macrophage polarization

The results described above indicate that hyperglycemia promotes macrophage polarization to the M1 phenotype, however, the associated mechanism remains unclear. To evaluate Notch activity in pancreases from each group, Rbpj immunostaining was performed. Higher Rbpj staining was observed in acinar-to-ductal metaplasia (ADM) structures and interstitial infiltrations in AP than CON pancreases (Figure 4A). In addition, pancreases from the APG3d and APG7d groups had significantly more Rbpj positive cells than pancreases from the AP3d and AP7d groups (Figure 4A,B), suggesting that hyperglycemic condition further elevated Notch activity after AP. Western blot analysis also showed significantly higher Rbpj and Hes1 levels in pancreatic tissues from APG versus AP mice (Figure 4C–E). To investigate the impact of Notch up-regulation on macrophage polarization, immunofluorescent costaining of Hes1 and CD68 was performed. $CD68^{+}Hes1^{+}$ macrophages were markedly higher in AP than CON pancreases, and the proportion of co-expressing cells was significantly higher in the APG groups than the corresponding AP groups (Figure 4F,G). These results show that the increased M1 polarization that occurs under hyperglycemic conditions may be associated with up-regulated Notch signaling.

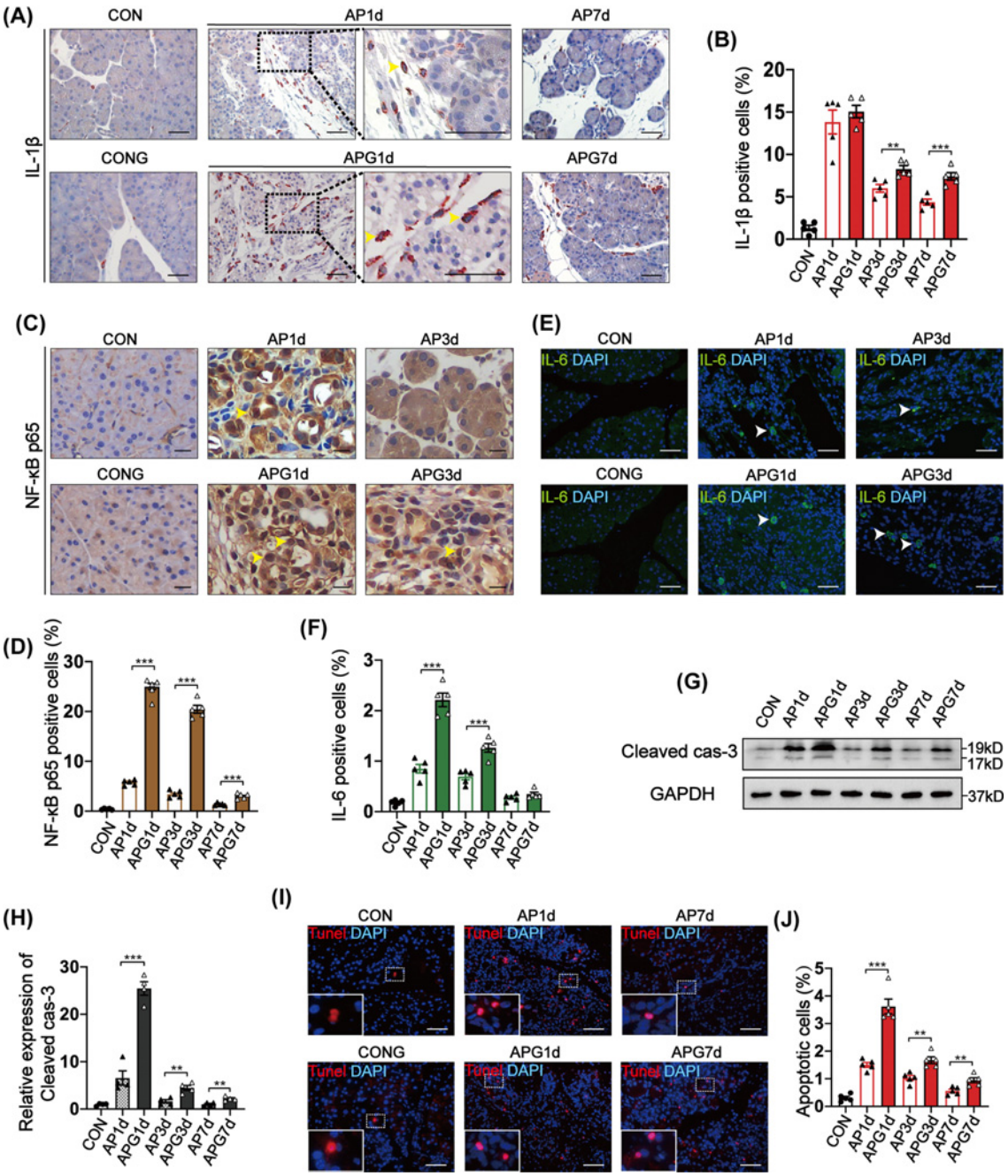

Figure 2. Hyperglycemia exacerbates inflammation and increases apoptosis following AP

(**A**) Staining of IL-1β in the pancreases from CON, CONG, AP, and APG mice. Arrowheads indicate the IL-1β positive cells. (**B**) Quantification of IL-1β positive cells at indicated time points under 400× magnification (shown as %). (**C**) NF-κB p65 staining in the pancreases of CON, CONG, AP, and APG mice. Arrowheads refer to NF-κB p65 positive cells. (**D**) Quantification of NF-κB p65 positive cells in CON, AP, and APG pancreases under 400× magnification at indicated time points (shown as %). (**E**) Representative images of the pancreases from CON, CONG, AP, and APG groups that were immunostained for IL-6 (green) and DAPI (blue). Arrowheads indicate the IL-6 positive cells. (**F**) Quantification of IL-6 positive cells in CON, AP, and APG pancreases under 400× magnification at indicated time points (shown as %). (**G**) Representative Western blots of cleaved caspase-3 in pancreases from CON, AP, and APG mice. (**H**) Quantification of cleaved caspase-3 levels in AP and APG mouse pancreases compared with CON pancreases. (**I**) Representative images of pancreases from CON, CONG, AP, and APG mice stained for TUNEL (red) and DAPI (blue). (**J**) Quantification of TUNEL positive cells under 400× magnification (shown as %). Abbreviations: APG, acute pancreatitis with glucose treatment; CONG, control with glucose treatment. Data are presented as the mean ± SEM, n=4–5. $^{**}P<0.01$, $^{***}P<0.001$. Scale bars, 50 μm (A,E,I) and 20 μm (C).

Clinical Science (2022) **136** 455–471
https://doi.org/10.1042/CS20211031

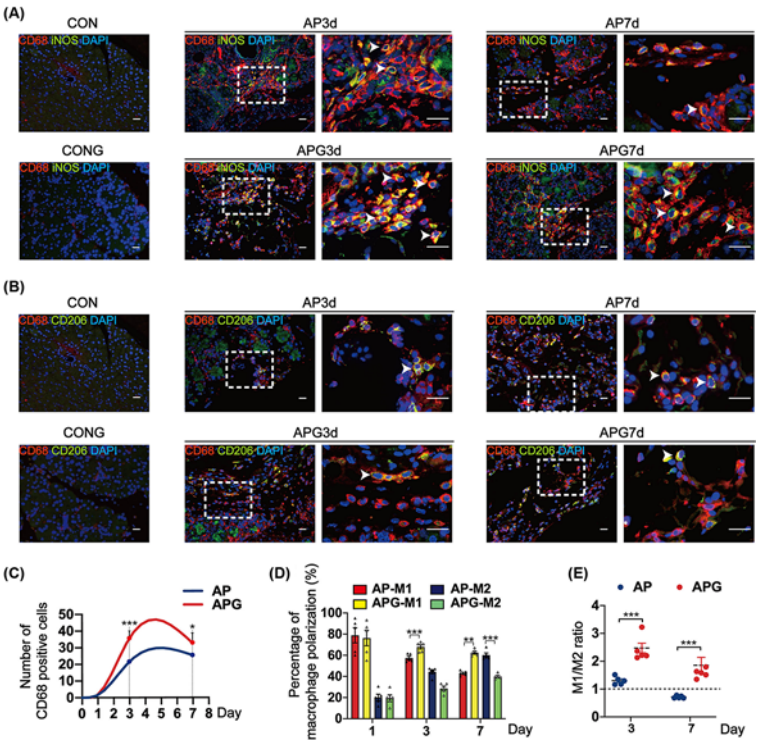

Figure 3. Hyperglycemia stimulates pancreatic macrophage polarization to an M1 phenotype during AP

(**A**) Representative images of CON, CONG, AP, and APG pancreases immunostained for CD68 (red), iNOS (green), and DAPI (blue) to identify M1 macrophages. Arrowheads indicate $CD68^+iNOS^+$ M1 macrophages. (**B**) Images of CON, CONG, AP, and APG mice pancreases immunostained for CD68 (red), CD206 (green), and DAPI (blue) to identify M2 macrophages. Arrowheads indicate the $CD68^+CD206^+$ M2 macrophages. (**C**) Quantification of macrophage infiltration in AP and APG mice pancreases at indicated time points under 400× magnification. (**D**) Quantification of M1 and M2 macrophage percentages in AP and APG mouse pancreases at indicated time points. (**E**) The ratio of the macrophage phenotype was calculated as M1/M2. Abbreviation: APG, acute pancreatitis with glucose treatment; CONG, control with glucose treatment. Data are presented as the mean ± SEM, n=5. $^*P<0.05$, $^{**}P<0.01$, $^{***}P<0.001$. Scale bars, 20 μm.

DAPT inhibits hyperglycemia-augmented Notch activity and M1 polarization *in vitro*

To investigate the role of Notch signaling in macrophage polarization *in vitro*, BMDMs (Figure 5A) and pancreatic acinar cells were isolated from FVB/N mice, and CD68 immunostaining was used to identify isolated macrophages after a 7-day M-CSF stimulation. A co-incubation system using BMDMs and cerulein-stimulated acinar cells was established. In brief, pancreatic acini were treated with cerulein to simulate the pancreatitis model, and the cerulein-stimulated acini were transferred to the co-culture system to cultivate BMDMs (Figure 5B). While acini-stimulated BMDMs showed robust Notch activity, the administration of the Notch signaling inhibitor, DAPT, to the co-culture system significantly reduced macrophage Notch activity in a dose-dependent manner as shown by reduced Rbpj and Hes1 levels (Figure 5C–E).

To further explore the impact of hyperglycemia on macrophage polarization, different concentrations of glucose were added to the co-culture system. Notch1, Notch2, and Rbpj mRNA levels in the macrophages increased significantly after culture with cerulein-stimulated acini and rose even higher after hyperglycemia was induced. However, the addition of DAPT (40 μM) to the co-culture system successfully reduced Notch1, Notch2, and Rbpj mRNA levels (Figure 5F–H). Western blot analysis also showed significantly higher Rbpj and Hes1 protein levels in macrophages after high concentration glucose treatment, while blocking Notch signaling with DAPT reversed this phenomenon (Figure 5I–K). Levels of M1 macrophage cytokines, IL-1β, IL-6, and TNF-α, increased significantly in macrophages in the co-culture system, and cytokine mRNA levels further increased under hyperglycemic conditions, indicating that hyperglycemia increased M1 polarization. DAPT significantly reduced the expression of these cytokines, suggesting that polarization towards the M1 phenotype was inhibited by Notch suppression (Figure 5L–N).

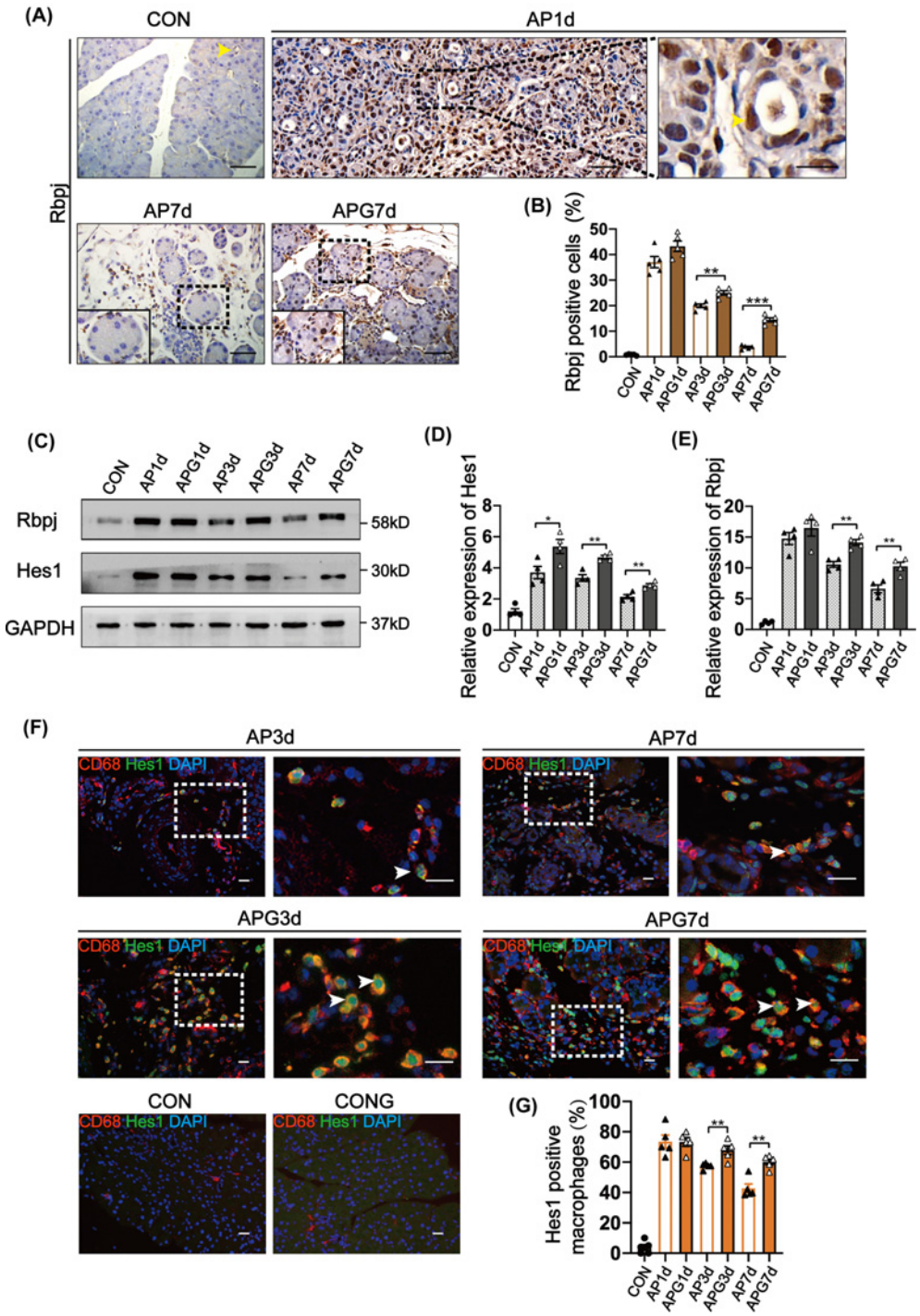

Figure 4. Notch activity is augmented under hyperglycemic conditions during AP and is associated with macrophage polarization

(**A**) Staining of Rbpj in pancreases from CON, AP1d, AP7d, and APG7d mice. Arrowheads indicate Rbpj positive cells. (**B**) Quantification of Rbpj positive cells in pancreases from CON, AP, and APG mice at indicated time points (shown as %). (**C**) Representative Western blots of Rbpj and Hes1 from CON, AP, and APG mice pancreases. (**D**,**E**) Quantification of Western blots for Rbpj and Hes1 expression in AP and APG pancreases relative to control pancreases. (**F**) Representative images of pancreases immunostained with CD68 (red), Hes1 (green), and DAPI (blue) showing Hes1 expression in pancreatic macrophages. Arrowheads indicate $CD68^{+}Hes1^{+}$ macrophages. (**G**) Quantification of $CD68^{+}Hes1^{+}$ macrophages in each group (shown as %). Abbreviations: APG, acute pancreatitis with glucose treatment; CONG, control with glucose treatment. Data are presented as the mean ± SEM, n=4–5. $^{*}P<0.05$, $^{**}P<0.01$, $^{***}P<0.001$. Scale bars, 50 μm (A) and 20 μm (right graph of (A),(F)).

Clinical Science (2022) **136** 455–471
https://doi.org/10.1042/CS20211031

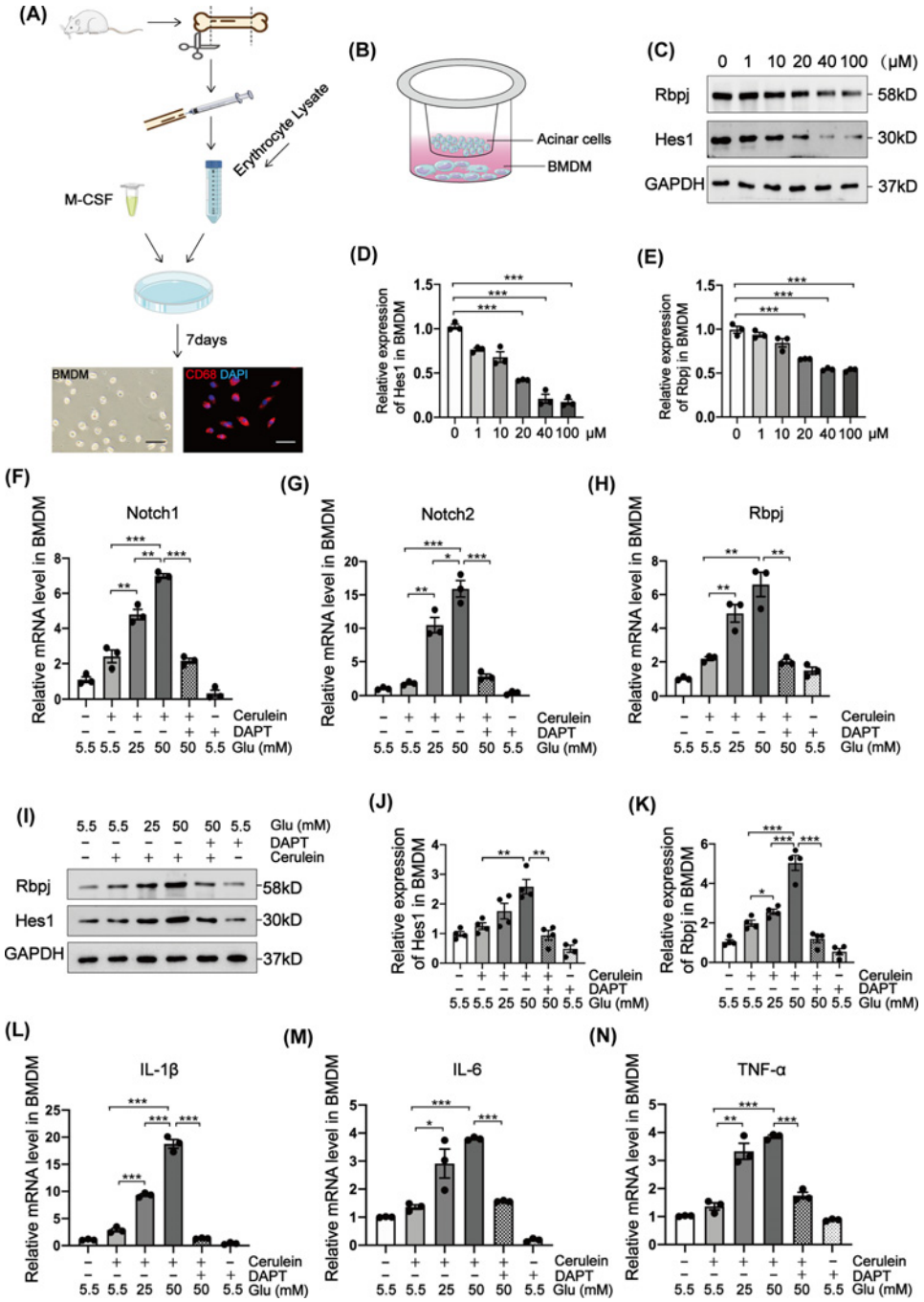

Figure 5. DAPT inhibits hyperglycemia-induced augmentation of Notch activity and the release of inflammatory factors from macrophages

(**A**) Schematic diagram of BMDMs isolation, and identification of M0 macrophages after M-CSF induction by immunofluorescent staining with CD68 (red) and DAPI (blue). (**B**) Schematic depicting the co-cultivation of pancreatic acinar cells and macrophages. (**C**) Representative Western blots of Rbpj and Hes1 expression in macrophages after supplementation with different DAPT concentrations. (**D**,**E**) Western blots quantification of Rbpj and Hes1 in macrophages following DAPT treatment. (**F**–**H**) Macrophages were co-cultured with cerulein-stimulated acini in the medium supplemented with different glucose concentrations and collected after 4 days to analyze Notch1, Notch2, and Rbpj mRNA levels. (**I**) Western blots of Rbpj and Hes1 expression in co-cultured macrophages under specified conditions. (**J**,**K**) Quantification of Western blots for Rbpj and Hes1 in co-cultured macrophages under specified conditions. (**L**–**N**) IL-1β, IL-6, and TNF-α mRNA levels in co-cultured macrophages under specified conditions. Data are presented as the mean ± SEM, n=3–4 experiments; each experiment was performed using cells from independent primary cell isolation. *P<0.05, **P<0.01, ***P<0.001. Scale bars, 20 μm.

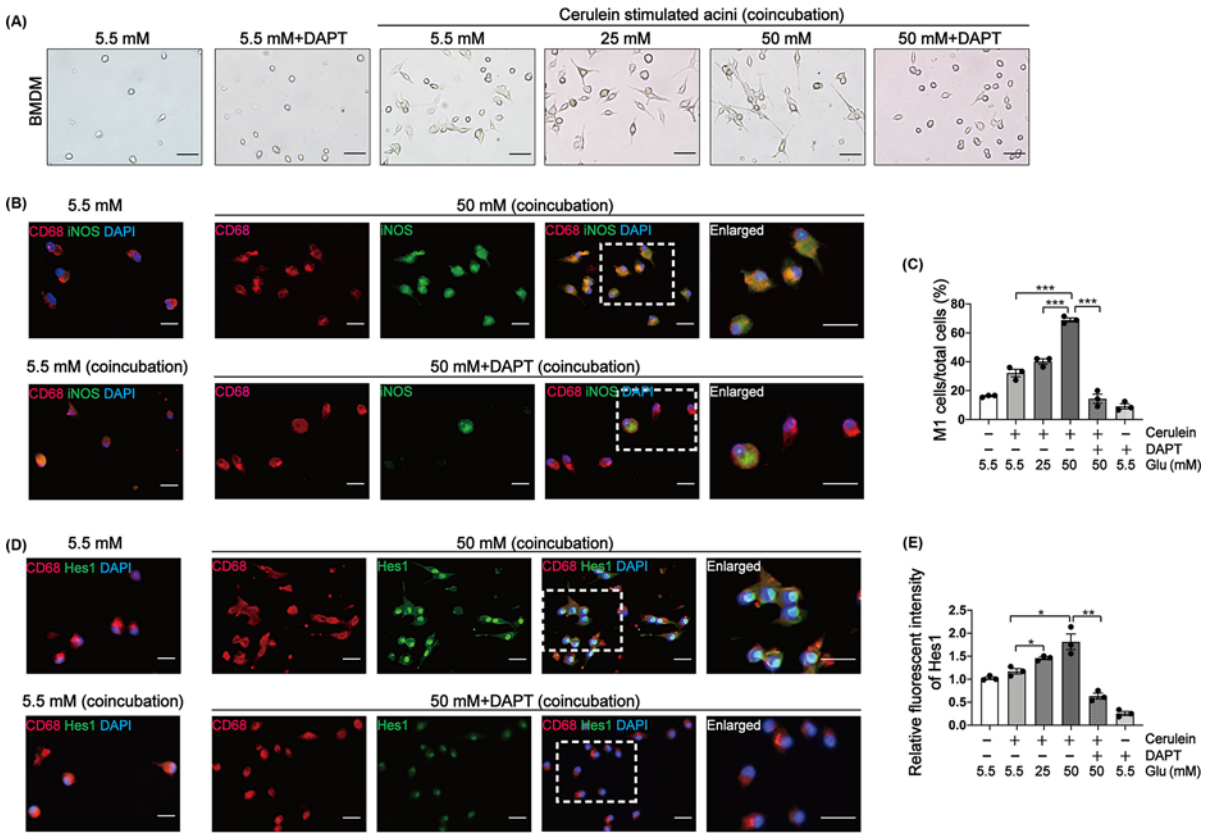

Figure 6. DAPT inhibits the polarization of macrophages towards an M1 phenotype

(**A**) Morphological changes of macrophages in the co-culture system under specified conditions. (**B**) Immunofluorescent staining of macrophages with CD68 (red), iNOS (green), and DAPI (blue), to identify M1 macrophages. (**C**) Quantification of $CD68^{+}iNOS^{+}$ M1 macrophages (shown as %). (**D**) Immunofluorescent staining of macrophages with CD68 (red), Hes1 (green), and DAPI (blue), to evaluate Notch activity. (**E**) Relative fluorescent intensity of Hes1 in macrophages from each indicated group. Data are presented as the mean ± SEM, n=3 experiments; each experiment was performed using cells from independent primary cell isolation. $^{*}P<0.05$, $^{**}P<0.01$, $^{***}P<0.001$. Scale bars, 50 μm (A) and 20 μm (B,D).

Assessment of cellular morphology showed that some macrophages developed a fusiform shape after coculture with cerulein-stimulated acinar cells, suggesting that polarization had occurred. High concentration glucose insult further promoted changes to macrophage morphology, while DAPT treatment inhibited morphology changes (Figure 6A). Immunostaining of CD68 and either Hes1 or iNOS showed significant increase in macrophage Notch activity and increased M1 polarization in the co-culture system following high concentration glucose stimulation, while DAPT treatment reduced both phenomena (Figure 6B–E). These findings suggest that up-regulated macrophage Notch activity in hyperglycemic conditions promoted macrophage polarization towards an M1 phenotype.

Knockdown of Notch1 attenuates LPS-induced M1 polarization and release of proinflammatory factors from RAW264.7 cells

Lentivirus transfection was used to knockdown Notch1 in RAW264.7 cells in order to further verify the role of Notch signaling in macrophage polarization. Fluorescent images 48 h after lentivirus transfection are shown in Figure 7A. Notch1 mRNA levels, and Rbpj and Hes1 protein levels decreased significantly after Notch1 knockdown (Figure 7B–E), suggesting that Notch activity was effectively inhibited. To mimic inflammation in RAW264.7 cells, a series of exogenous LPS concentrations were administered. After LPS stimulation for 24 h, Notch activity and TNF-α production in RAW264.7 cells increased in a dose-dependent manner (Figure 7F,G). Thus, 1 μmol/ml LPS was selected for the subsequent experiment. The hyperglycemic condition was established using 50 mM glucose stimulation. For the CON-RAW264.7 cells, LPS stimulation significantly increased Notch1, Hes1, and Rbpj mRNA, and Hes1 and Rbpj protein levels, and expression was further increased under hyperglycemic conditions. Notch1, Hes1,

Clinical Science (2022) **136** 455–471
https://doi.org/10.1042/CS20211031

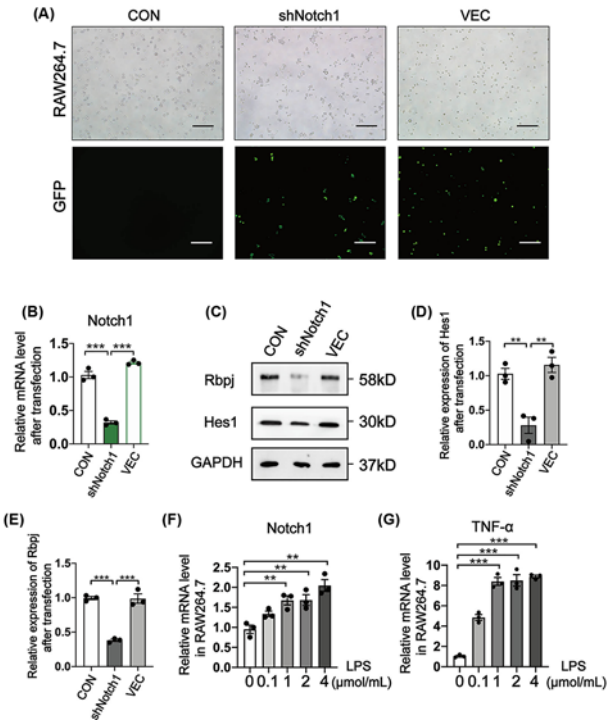

Figure 7. Knockdown of Notch1 by lentivirus transfection and LPS stimulation of RAW264.7 cells

(**A**) Representative bright-field and fluorescent images of RAW264.7 after 48 h of lentivirus transfection. (**B**) Notch1 mRNA levels of RAW264.7 cells in CON, shNotch1, and VEC groups. (**C**) Representative Western blots of Rbpj and Hes1 expression in CON, shNotch1, and VEC groups of RAW264.7 cells. (**D**,**E**) Western blots quantification of Rbpj and Hes1 protein levels in RAW264.7 cells from the CON, shNotch1, and VEC groups. (**F**,**G**) Notch1 and TNF-α mRNA levels in RAW264.7 cells after stimulation with different concentrations of LPS for 24 h. Abbreviations: CON, control; shNotch1, short hairpin RNA to knockdown Notch1; VEC, vector. Data are presented as the mean ± SEM, n=3 experiments. $^{**}P<0.01$, $^{***}P<0.001$. Scale bars, 200 μm.

and Rbpj mRNA, and Hes1 and Rbpj protein levels were significantly lower in Notch1 knockdown RAW264.7 cells than CON-RAW264.7 cells (Figure 8A–F). IL-1β, IL-6, and TNF-α mRNA, and IL-6 and TNF-α protein levels were significantly higher after LPS and high-concentration glucose treatment of CON-RAW264.7 cells than Notch1 knockdown RAW264.7 cells (Figure 8D,G–K). To quantify the number of M1 macrophages, iNOS protein levels were measured in each group. LPS treatment significantly increased iNOS expression in CON-RAW264.7 cells, and hyperglycemia further elevated iNOS. However, iNOS protein levels were lower in Notch1 knockdown RAW264.7 cells than CON-RAW264.7 cells in response to the indicated treatment (Figure 8L,M). These findings suggest that inhibition of Notch activity via Notch1 knockdown in RAW264.7 cells prevented LPS and hyperglycemia-induced M1 polarization of macrophages.

Discussion

In the present study, a cerulein-induced AP model with hyperglycemia was established. Animal experiments demonstrated that hyperglycemic conditions aggravated the pancreatic injury, promoted M1 polarization, and elevated Notch signaling following AP. *In vitro* experiments confirmed that hyperglycemia facilitated M1 polarization by amplifying Notch signaling in macrophages. Inhibition of Notch signaling of macrophages by DAPT or Notch1 knockdown prevented M1 polarization and decreased the production of proinflammatory factors. These data suggest that hyperglycemia conditions can aggravate AP and controlling blood glucose or inhibiting Notch signaling during early AP may prevent progression to severe disease.

Although studies have assessed the impact of diabetes on the progression of AP, the role of hyperglycemia in AP patients remains poorly understood. In clinical practice, hyperglycemia is observed in most patients with AP, potentially resulting from an acute stress response that activates the neuroendocrine system and causes the release of glucagon [30,31]. In addition, AP-induced β-cell injury reduces insulin secretion [32], and the complex interplay

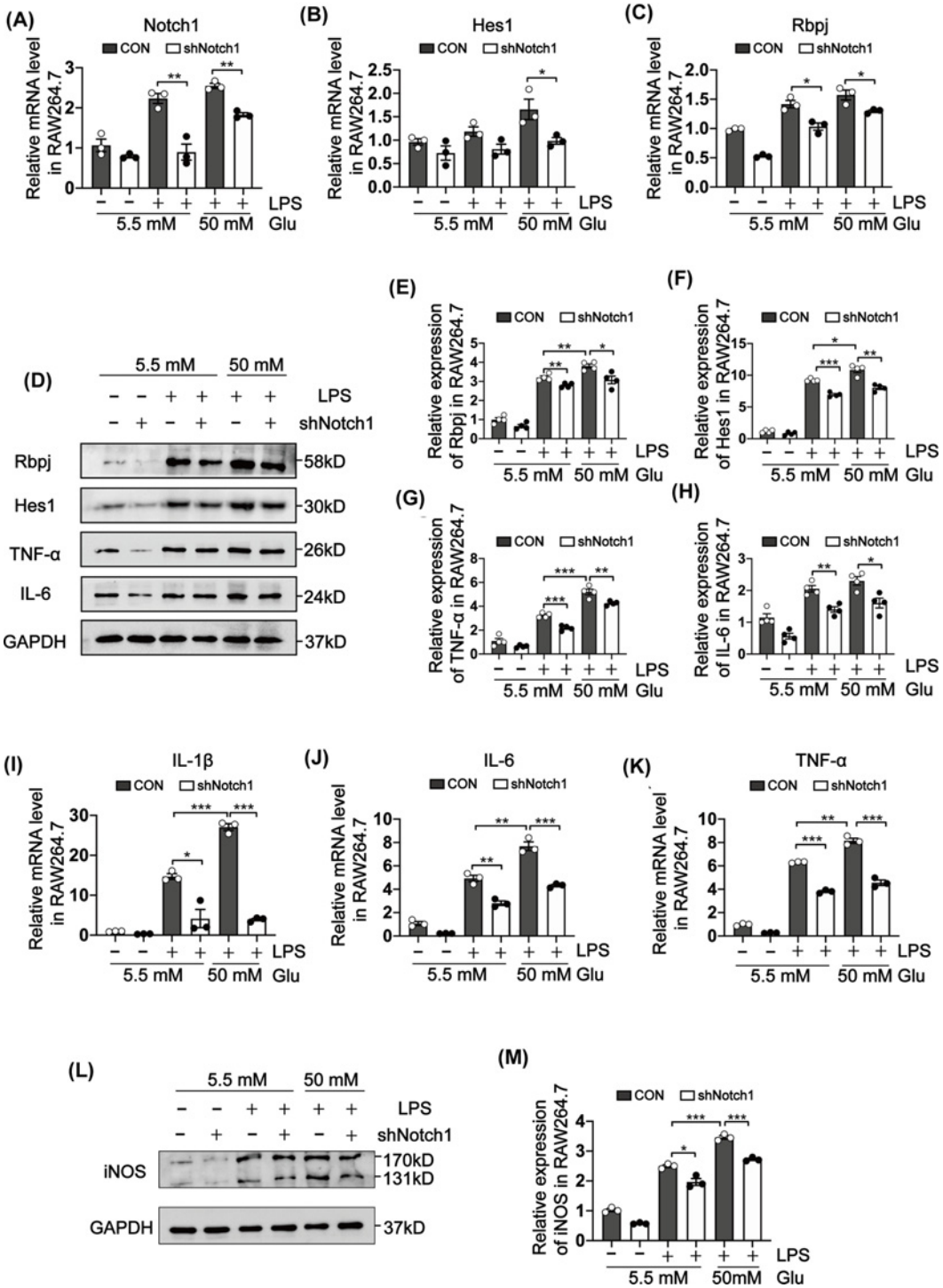

Figure 8. Knockdown of Notch1 attenuates LPS- and hyperglycemia-induced M1 polarization and the release of proinflammatory factors in RAW264.7 cells

(**A**–**C**) Notch1, Hes1, and Rbpj mRNA in CON and shNotch1 RAW264.7 cells. (**D**) Representative Western blots of Rbpj, Hes1, TNF-α, and IL-6 expression in RAW264.7 cells (CON and shNotch1 groups) under specified conditions. (**E**–**H**) Quantification of Western blots for Rbpj, Hes1, TNF-α, and IL-6 in CON and shNotch1 RAW264.7 cells under specified conditions. (**I**–**K**) IL-1β, IL-6, and TNF-α mRNA in CON and shNotch1 RAW264.7 cells. (**L**) Representative Western blot of iNOS in CON and shNotch1 RAW264.7 cells under indicated conditions. (**M**) Western blot quantification of iNOS in CON and shNotch1 RAW264.7 cells. Abbreviation: shNotch1, short hairpin RNA to knockdown Notch1. Data are presented as the mean ± SEM, n=3–4 experiments. $^{*}P<0.05$, $^{**}P<0.01$, $^{***}P<0.001$.

Clinical Science (2022) **136** 455–471
https://doi.org/10.1042/CS20211031

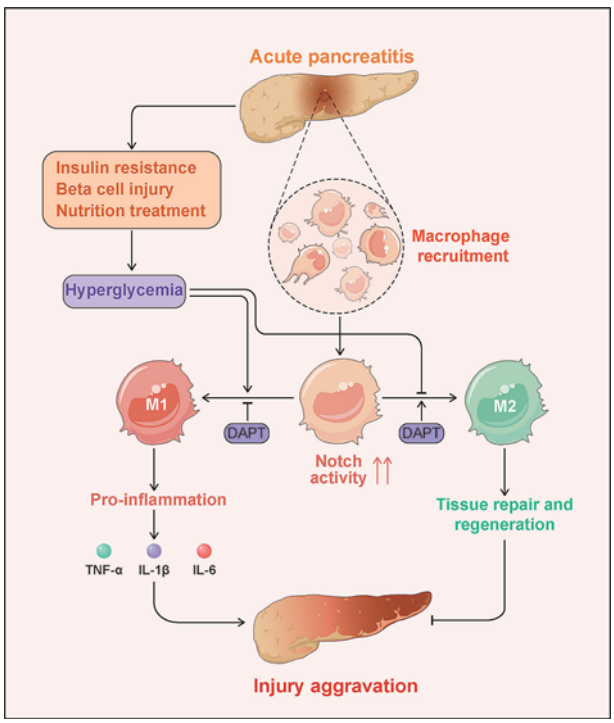

Figure 9. Diagram of the role of hyperglycemia-augmented Notch signaling in pancreatic macrophage polarization during AP

Macrophages are recruited into the pancreas and polarize into M1/M2 phenotypes, and Notch signaling is activated during AP. Hyperglycemia may be induced by multiple factors during AP. Hyperglycemia-augmented Notch activity promotes macrophage polarization towards an M1 phenotype and aggravates pancreatic injury. Inhibition of Notch activity may decrease the number of proinflammatory M1 macrophages and alleviate AP.

between multiple hormones and cytokines causes insulin resistance, which further aggravates hyperglycemia [31]. Enteral and parenteral nutrition treatment during AP can also induce transient hyperglycemia [9].

Previous studies have shown that diabetes aggravates AP and AP diabetic mice receiving insulin treatment have less cell death and increased expansion of acinar cells [33–35]. The current study focused on the impact of hyperglycemia on pancreatitis during early AP, rather than diabetes. Acute hyperglycemia was shown to aggravate pancreatic injury and inflammatory infiltration, and increase acinar cell apoptosis following AP. Interestingly, hyperglycemia increased the number of macrophages that infiltrated the pancreatic parenchyma, promoted M1 polarization, inhibited M2 polarization, and increased the release of proinflammatory factors. Macrophages are important innate immune cells in mice and humans, and the balance of M1 and M2 macrophages plays a critical role in regulating the immune response [36]. Hyperglycemia is shown to exacerbate hepatic ischemia/reperfusion injury by promoting M1 polarization and inhibiting M2 polarization, further supporting the findings from the current study [37].

Notch signaling is pivotal to the development and differentiation of progenitor cells in the embryonic pancreas [38], and plays a decisive role in the differentiation of multiple cell lineages including dendritic cells and macrophages [39]. Prior studies have demonstrated a role for Notch signaling in the regulation of inflammation and apoptosis [40,41]. Available data confirm that Notch signaling is activated in the cerulein-induced AP model, and previous research has shown that Notch activity is elevated in the injured pancreases of AP patients and essential to the regeneration of impaired pancreatic acinar cells during AP [26,42,43]. However, excessively activated Notch signaling is harmful and is shown to aggravate renal podocyte injury in mouse models of diabetic and adriamycin-induced nephropathy [44]. Other studies have demonstrated that Notch signaling can aggravate hypoxia/reoxygenation-induced cardiomyocyte injury [45]. These studies suggest that excessively activated Notch signaling can aggravate organ or tissue injury in multiple disease models. It also has been shown that the Notch-Rbpj pathway selectively regulates M1 macrophage-associated gene expression in LPS-induced BMDMs injury [46]. In a bacterial infection model, up-regulation of macrophage Notch signaling promotes macrophage polarization towards an M1 phenotype, resulting in increased production of inflammatory factors and aggravating tissue damage [47]. In the AP model described

in the current study, Notch signaling was activated in pancreatic macrophages, and the hyperglycemic condition further increased Notch activity and promoted macrophage polarization towards an M1 phenotype. DAPT treatment or Notch1 knockdown in primary macrophages and macrophage cell lines depressed M1 polarization and decreased the production of proinflammatory factors. These data suggest that Notch signaling is a potential target for the prevention and treatment of AP.

Conclusions

The present study demonstrates that hyperglycemia promotes macrophage polarization towards an M1 phenotype, increases the production of proinflammatory factors, and aggravates pancreatic injury during AP, all of which are associated with higher Notch signaling. These results provide evidence that controlling blood glucose is critical for the effective treatment of AP. The present study reveals a novel mechanism for Notch signaling in AP and provides a molecular basis for AP treatment.

Clinical perspectives

- Most patients with AP suffer from hyperglycemia. Previous research indicates that Notch signaling is increased in the injured pancreases of AP patients but it remains unclear whether hyperglycemia impacts pancreatic Notch signaling and disease severity after AP.
- Findings from the present study suggest that hyperglycemia promotes pancreatic macrophage polarization to the M1 phenotype during AP. Inhibiting Notch activity prevents M1 polarization and mitigates pancreatic injury after AP.
- The present study shows that reduced Notch activity and well-controlled blood glucose are necessary to prevent AP disease progression, and Notch signaling may be a potential target for the treatment of AP. Further studies are required to establish clinical evidence.

Data Availability

Data presented in this manuscript are available upon reasonable request from the corresponding authors.

Competing Interests

The authors declare that there are no competing interests associated with the manuscript.

Funding

This work was supported by the National Natural Science Foundation of China [grant numbers 81800574, 82170651 (to Qiao Shi) and 81870442 (to Weixing Wang)].

CRediT Author Contribution

Ning Hu: Data curation, Investigation, Methodology, Writing—original draft. **Xiaoyi Zhang:** Data curation, Investigation, Methodology, Writing—original draft. **Xuanzhe Zhang:** Data curation, Investigation, Methodology. **Yongjun Guan:** Investigation, Methodology. **Ruyuan He:** Investigation. **Enfu Xue:** Investigation. **Xiaoyi Zhang:** Investigation. **Wenhong Deng:** Investigation. **Jia Yu:** Investigation. **Weixing Wang:** Conceptualization, Funding acquisition, Writing—review & editing. **Qiao Shi:** Conceptualization, Funding acquisition, Data curation, Investigation, Writing—review & editing.

Abbreviations

AP, acute pancreatitis; BMDM, bone marrow-derived macrophage; CON, control; DAB, diaminobezidin; DAPT, N-[N-(3,5-Difluorophenacetyl)-L-alanyl]-S-phenylglycine t-butyl ester; DMEM, Dulbecco's modified Eagle's medium; FBS, fetal bovine serum; GAPDH, glyceraldehyde-3-phosphate dehydrogenase; HRP, horseradish peroxidase; IL, interleukin; iNOS, inducible nitric oxide synthase; LPS, lipopolysaccharide; M-CSF, macrophage colony-stimulating factor; NF-κB p65, nuclear factor κ-B p65; P/S, Penicillin–Streptomycin; PBS, phosphate-buffered saline; qRT-PCR, quantitative real-time polymerase chain reaction; Rbpj, Recombination signal binding protein for immunoglobulin kappa J region; TNF-α, tumor necrosis factor-α; TUNEL, terminal deoxynucleotidyl transferase-mediated dUTP-biotin nick end labeling.

Clinical Science (2022) **136** 455–471
https://doi.org/10.1042/CS20211031

References

1 Lankisch, P.G., Apte, M. and Banks, P.A. (2013) Acute pancreatitis. *Lancet* **386**, 85–96, https://doi.org/10.1016/S0140-6736(14)60649-8

2 Xiao, A.Y., Tan, M.L., Wu, L.M., Asrani, V.M., Windsor, J.A., Yadav, D. et al. (2016) Global incidence and mortality of pancreatic diseases: a systematic review, meta-analysis, and meta-regression of population-based cohort studies. *Lancet Gastroenterol. Hepatol.* **1**, 45–55, https://doi.org/10.1016/S2468-1253(16)30004-8

3 Lee, P.J. and Papachristou, G.I. (2019) New insights into acute pancreatitis. *Nat. Rev. Gastroenterol. Hepatol.* **16**, 479–496, https://doi.org/10.1038/s41575-019-0158-2

4 Banks, P.A., Bollen, T.L., Dervenis, C., Gooszen, H.G., Johnson, C.D., Sarr, M.G. et al. (2013) Classification of acute pancreatitis–2012: revision of the Atlanta classification and definitions by international consensus. *Gut* **62**, 102–111, https://doi.org/10.1136/gutjnl-2012-302779

5 Tenner, S., Baillie, J., DeWitt, J., Vege, S.S. and American College of Gastroenterology (2013) American College of Gastroenterology guideline: management of acute pancreatitis. *Am. J. Gastroenterol.* **108**, 1400–1415, https://doi.org/10.1038/ajg.2013.218

6 Machicado, J.D., Gougol, A., Paragomi, P., OKeefe, S.J., Lee, K., Slivka, A. et al. (2018) Practice patterns and utilization of tube feedings in acute pancreatitis patients at a large US referral center. *Pancreas* **47**, 1150–1155, https://doi.org/10.1097/MPA.0000000000001141

7 Shi, Q., Hong, Y.P., Zhang, X.Y., Tao, J., Wang, C.Y., Zhao, L. et al. (2018) β cells can be generated from cytokeratin 5-positive cells after cerulein-induced pancreatitis in adult mice. *Biochem. Biophys. Res. Commun.* **496**, 114–119, https://doi.org/10.1016/j.bbrc.2018.01.008

8 Shenoy, S.D., Cody, D., Rickett, A.B. and Swift, P.G. (2004) Acute pancreatitis and its association with diabetes mellitus in children. *J. Pediatr. Endocrinol. Metab.* **17**, 1667–1670, https://doi.org/10.1515/JPEM.2004.17.12.1667

9 Petrov, M.S. and Whelan, K. (2010) Comparison of complications attributable to enteral and parenteral nutrition in predicted severe acute pancreatitis: a systematic review and meta-analysis. *Br. J. Nutr.* **103**, 1287–1295, https://doi.org/10.1017/S0007114510000887

10 Bharmal, S.H., Pendharkar, S., Singh, R.G., Cho, J. and Petrov, M.S. (2019) Glucose counter-regulation after acute pancreatitis. *Pancreas* **48**, 670–681, https://doi.org/10.1097/MPA.0000000000001318

11 Shen, H.N., Chang, Y.H., Chen, H.F., Lu, C.L. and Li, C.Y. (2012) Increased risk of severe acute pancreatitis in patients with diabetes. *Diabetes Med.* **29**, 1419–1424, https://doi.org/10.1111/j.1464-5491.2012.03680.x

12 Gordon, S. and Taylor, P.R. (2005) Monocyte and macrophage heterogeneity. *Nat. Rev. Immunol.* **5**, 953–964, https://doi.org/10.1038/nri1733

13 Mosser, D.M. and Edwards, J.P. (2008) Exploring the full spectrum of macrophage activation. *Nat. Rev. Immunol.* **8**, 958–969, https://doi.org/10.1038/nri2448

14 Wu, J., Zhang, L., Shi, J., He, R., Yang, W., Habtezion, A. et al. (2020) Macrophage phenotypic switch orchestrates the inflammation and repair/regeneration following acute pancreatitis injury. *EBioMedicine* **58**, 102920, https://doi.org/10.1016/j.ebiom.2020.102920

15 Lejay, A., Fang, F., John, R., Van, J.A., Barr, M., Thaveau, F. et al. (2016) Ischemia reperfusion injury, ischemic conditioning and diabetes mellitus. *J. Mol. Cell Cardiol.* **91**, 11–22, https://doi.org/10.1016/j.yjmcc.2015.12.020

16 Wanrooy, B.J., Kumar, K.P., Wen, S.W., Qin, C.X., Ritchie, R.H. and Wong, C.H.Y. (2018) Distinct contributions of hyperglycemia and high-fat feeding in metabolic syndrome-induced neuroinflammation. *J. Neuroinflammation* **15**, 1–13, https://doi.org/10.1186/s12974-018-1329-8

17 Wang, Q., Wei, S., Zhou, S., Qiu, J., Shi, C., Liu, R. et al. (2020) Hyperglycemia aggravates acute liver injury by promoting liver-resident macrophage NLRP3 inflammasome activation via the inhibition of AMPK/mTOR-mediated autophagy induction. *Immunol. Cell Biol.* **98**, 54–66, https://doi.org/10.1111/imcb.12297

18 Radtke, F., Fasnacht, N. and Macdonald, H.R. (2010) Notch signaling in the immune system. *Immunity* **32**, 14–27, https://doi.org/10.1016/j.immuni.2010.01.004

19 Siebel, C. and Lendahl, U. (2017) Notch signaling in development, tissue homeostasis, and disease. *Physiol. Rev.* **97**, 1235–1294, https://doi.org/10.1152/physrev.00005.2017

20 Kageyama, R. and Ohtsuka, T. (1999) The Notch-Hes pathway in mammalian neural development. *Cell Res.* **9**, 179–188, https://doi.org/10.1038/sj.cr.7290016

21 Kopan, R. and Ilagan, M.X. (2009) The canonical notch signaling pathway: unfolding the activation mechanism. *Cell* **137**, 216–233, https://doi.org/10.1016/j.cell.2009.03.045

22 Bray, S.J. (2006) Notch signalling: a simple pathway becomes complex. *Nat. Rev. Mol. Cell Biol.* **7**, 678–689, https://doi.org/10.1038/nrm2009

23 Wang, Y.C., He, F., Feng, F., Liu, X.W., Dong, G.Y., Qin, H.Y. et al. (2010) Notch signaling determines the M1 versus M2 polarization of macrophages in antitumor immune responses. *Cancer Res.* **70**, 4840–4849, https://doi.org/10.1158/0008-5472.CAN-10-0269

24 Lin, Y., Zhao, J.L., Zheng, Q.J., Jiang, X., Tian, J., Liang, S.Q. et al. (2018) Notch signaling modulates macrophage polarization and phagocytosis through direct suppression of signal regulatory protein α expression. *Front. Immunol.* **9**, 1–12, https://doi.org/10.3389/fimmu.2018.01744

25 Miloudi, K., Oubaha, M., Ménard, C., Dejda, A., Guber, V., Cagnone, G. et al. (2019) NOTCH1 signaling induces pathological vascular permeability in diabetic retinopathy. *Proc. Natl. Acad. Sci. U.S.A.* **116**, 4538–4547, https://doi.org/10.1073/pnas.1814711116

26 Zhang, X., Tao, J., Yu, J., Hu, N., Zhang, X., Wang, G. et al. (2021) Inhibition of Notch activity promotes pancreatic cytokeratin 5-positive cell differentiation to beta cells and improves glucose homeostasis following acute pancreatitis. *Cell Death Dis.* **23**, 867, 12(10), https://doi.org/10.1038/s41419-021-04160-2

27 Sendler, M., Weiss, F.U., Golchert, J., Homuth, G., van den Brandt, C., Mahajan, U.M. et al. (2018) Cathepsin B-mediated activation of trypsinogen in endocytosing macrophages increases severity of pancreatitis in mice. *Gastroenterology* **154**, 704–718, https://doi.org/10.1053/j.gastro.2017.10.018

28 Bläuer, M., Laaninen, M., Sand, J. and Laukkarinen, J. (2016) Reciprocal stimulation of pancreatic acinar and stellate cells in a novel long-term in vitro co-culture model. *Pancreatology* **16**, 570–577, https://doi.org/10.1016/j.pan.2016.03.012

29 Schmidt, J., Rattner, D.W., Lewandrowski, K., Compton, C.C., Mandavilli, U., Knoefel, W.T. et al. (1992) A better model of acute pancreatitis for evaluating therapy. *Ann. Surg.* **215**, 44–56, https://doi.org/10.1097/00000658-199201000-00007

30 Yang, X., Zhang, R., Jin, T., Zhu, P., Yao, L., Li, L. et al. (2021) Stress hyperglycemia is independently associated with persistent organ failure in acute pancreatitis. *Dig. Dis. Sci.*, https://doi.org/10.1007/s10620-021-06982-8
31 Dungan, K.M., Braithwaite, S.S. and Preiser, J.C. (2009) Stress hyperglycaemia. *Lancet* **373**, 1798–1807, https://doi.org/10.1016/S0140-6736(09)60553-5
32 Abdel-Hakeem, E.A., Abdel-Hamid, H.A. and Abdel Hafez, S.M.N. (2020) The possible protective effect of Nano-Selenium on the endocrine and exocrine pancreatic functions in a rat model of acute pancreatitis. *J. Trace Elem. Med. Biol.* **60**, 126480, https://doi.org/10.1016/j.jtemb.2020.126480
33 Zechner, D., Spitzner, M., Bobrowski, A., Knapp, N., Kuhla, A. and Vollmar, B. (2012) Diabetes aggravates acute pancreatitis and inhibits pancreas regeneration in mice. *Diabetologia* **55**, 1526–1534, https://doi.org/10.1007/s00125-012-2479-3
34 Mentula, P., Kylänpää, M.L., Kemppainen, E. and Puolakkainen, P. (2008) Obesity correlates with early hyperglycemia in patients with acute pancreatitis who developed organ failure. *Pancreas* **36**, 21–25, https://doi.org/10.1097/mpa.0b013e31814b22b5
35 Gao, L., Lu, G.T., Lu, Y.Y., Xiao, W.M., Mao, W.J., Tong, Z.H. et al. (2018) Diabetes aggravates acute pancreatitis possibly via activation of NLRP3 inflammasome in db/db mice. *Am. J. Transl. Res.* **10**, 2015–2025
36 Calderon, B., Carrero, J.A., Ferris, S.T., Sojka, D.K., Moore, L., Epelman, S. et al. (2015) The pancreas anatomy conditions the origin and properties of resident macrophages. *J. Exp. Med.* **212**, 1497–1512, https://doi.org/10.1084/jem.20150496
37 Hu, Y., Yang, C., Shen, G., Yang, S., Cheng, X., Cheng, F. et al. (2019) Hyperglycemia-triggered sphingosine-1-phosphate and sphingosine-1-phosphate receptor 3 signaling worsens liver ischemia/reperfusion injury by regulating M1/M2 polarization. *Liver Transplant.* **25**, 1074–1090, https://doi.org/10.1002/lt.25470
38 Afelik, S., Qu, X., Hasrouni, E., Bukys, M.A., Deering, T., Nieuwoudt, S. et al. (2012) Notch-mediated patterning and cell fate allocation of pancreatic progenitor cells. *Development* **139**, 1744–1753, https://doi.org/10.1242/dev.075804
39 Shang, Y., Smith, S. and Hu, X. (2016) Role of Notch signaling in regulating innate immunity and inflammation in health and disease. *Protein Cell* **7**, 159–174, https://doi.org/10.1007/s13238-016-0250-0
40 Piggott, K., Deng, J., Warrington, K., Younge, B., Kubo, J.T., Desai, M. et al. (2011) Blocking the NOTCH pathway inhibits vascular inflammation in large-vessel vasculitis. *Circulation* **123**, 309–318, https://doi.org/10.1161/CIRCULATIONAHA.110.936203
41 Kim, D., Lim, S., Park, M., Choi, J., Kim, J., Han, H. et al. (2014) Ubiquitination-dependent CARM1 degradation facilitates Notch1-mediated podocyte apoptosis in diabetic nephropathy. *Cell. Signal.* **26**, 1774–1782, https://doi.org/10.1016/j.cellsig.2014.04.008
42 Gomez, G., Englander, E.W., Wang, G. and Greeley, G.H.Jr. (2004) Increased expression of hypoxia-inducible factor-1α, p48, and the Notch signaling cascade during acute pancreatitis in mice. *Pancreas* **28**, 58–64, https://doi.org/10.1097/00006676-200401000-00009
43 Siveke, J.T., Lubeseder-Martellato, C., Lee, M., Mazur, P.K., Nakhai, H., Radtke, F. et al. (2008) Notch signaling is required for exocrine regeneration after acute pancreatitis. *Gastroenterology* **134**, 544–555, https://doi.org/10.1053/j.gastro.2007.11.003
44 Liu, M., Liang, K., Zhen, J., Zhou, M., Wang, X., Wang, Z. et al. (2017) Sirt6 deficiency exacerbates podocyte injury and proteinuria through targeting Notch signaling. *Nat. Commun.* **8**, 413, https://doi.org/10.1038/s41467-017-00498-4
45 Zhu, P., Yang, M., He, H., Kuang, Z., Liang, M., Lin, A. et al. (2019) Curcumin attenuates hypoxia/reoxygenation-induced cardiomyocyte injury by downregulating Notch signaling. *Mol. Med. Rep.* **20**, 1541–1550, https://doi.org/10.3892/mmr.2019.10371
46 Xu, H., Zhu, J., Smith, S., Foldi, J., Zhao, B., Chung, A.Y. et al. (2012) Notch-RBP-J signaling regulates the transcription factor IRF8 to promote inflammatory macrophage polarization. *Nat. Immunol.* **13**, 642–650, https://doi.org/10.1038/ni.2304
47 Keewan, E. and Naser, S.A. (2020) Notch-1 signaling modulates macrophage polarization and immune defense against mycobacterium avium paratuberculosis infection in inflammatory diseases. *Microorganisms* **8**, 1–15, https://doi.org/10.3390/microorganisms8071006

Supplementary Figure 1

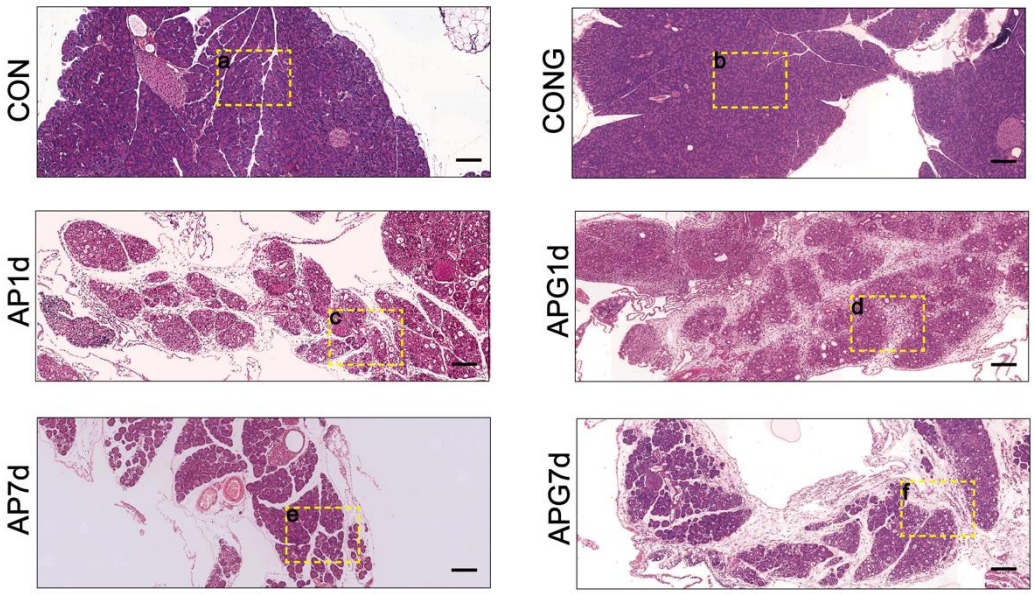

Supplementary Figure 1. Representative images of H&E staining of pancreases from CON, CONG, AP, and APG mice at indicated time points. AP, acute pancreatitis; APG, acute pancreatitis with glucose treatment; CON, control; CONG, control with glucose treatment; H&E, hematoxylin and eosin. Scale bars, 100 μm.

Supplementary Table

The histological score for each parameter assessed in each experimental group

Groups	Edema	Acinar necrosis	Hemorrhage	Fat necrosis	Inflammation infiltrate	Perivascular inflammation	Total
CON	0.400±0.100	0.020±0.012	0.050±0.050	0.050±0.050	0.260±0.024	0.040±0.010	0.820±0.137
CONG1d	0.300±0.122	0.030±0.020	0.100±0.100	0.100±0.100	0.230±0.078	0.100±0.027	0.860±0.083
AP1d	3.100±0.100	3.040±0.080	1.400±0.187	0.900±0.187	3.270±0.193	1.360±0.165	13.070±0.501
APG1d	3.200±0.122	3.220±0.101	1.400±0.245	1.400±0.187	3.300±0.167	1.800±0.170	14.320±0.616
CONG3d	0.500±0.158	0.040±0.024	0.150±0.100	0.200±0.200	0.050±0.039	0.060±0.019	1.000±0.239
AP3d	2.200±0.200	1.970±0.195	0.900±0.292	0.700±0.122	2.760±0.202	1.770±0.162	10.300±0.529
APG3d	2.300±0.200	1.830±0.098	2.000±0.247	1.200±0.200	3.520±0.041	2.190±0.195	13.040±0.464
CONG7d	0.600±0.187	0.030±0.012	0.100±0.061	0.100±0.100	0.080±0.041	0.040±0.029	0.950±0.097
AP7d	1.100±0.100	1.680±0.206	0.800±0.122	0.700±0.122	1.410±0.181	1.390±0.165	7.080±0.332
APG7d	1.200±0.200	1.750±0.372	1.200±0.200	1.100±0.187	1.890±0.086	1.650±0.122	8.790±0.549

Data are presented as the mean ± SEM. AP, acute pancreatitis; APG, acute pancreatitis with glucose treatment; CON, control; CONG, control with glucose treatment.